Rev. Adv. Mater. Sci. 32 (2012) 83-93

AN OVERVIEW OF THE EFFECTS OF CRYSTALLIZATION TIME, TEMPLATE AND SILICON SOURCES ON HYDROTHERMAL SYNTHESIS OF SAPO-34 MOLECULAR SIEVE WITH SMALL CRYSTALS

Sima Askari, Rouein Halladj and Morteza Sohrabi

Faculty of Chemical Engineering, Amirkabir University of Technology (Tehran Polytechnic), P.O. Box 15875-4413, Hafez Ave., Tehran, Iran

Received: November 07, 2011

Abstract. Several samples were synthesized under hydrothermal condition by using TEAOH (tetraethyl ammoniumhydroxide), DEA (diethylamine), TEA (triethylamine) and morpholine as structure-directing agents and TEOS and fumed silica as silicon sources. The significance of template, silicon sources and crystallization time on crystal phase, morphology, crystal size and crystallinity were studied and the results were compared with those of obtained from other investigations reported in this field. SAPO-5 and SAPO-34 with different crystal size in the range of 300 nm - 15 μm were formed, using different template and silicon sources. The SAPO crystals were characterized by X-ray diffraction (XRD), scanning electron microscopy (SEM), energy-dispersive X-ray spectroscopy (EDX), thermogravimetric analysis (TGA) and nitrogen adsorption technique (BET). The results show that TEAOH is the most proper template for SAPO-34 synthesis whereas TEA is an appropriate template for synthesis of SAPO-5. DEA and morpholine, however, can produce SAPO-34 or/and other phases depending on their concentration used. Using TEOS as silica source, results in producing finer particles with narrower size distribution for almost all samples. Crystallization time has a significant effect on crystal size and crystalliniy.

1. INTRODUCTION

Silicoaluminophosphates (SAPO) are an important class of molecular sieves which may possess Bronsted acidic sites with the substitution of Si into the neutral framework of $AlPO_4$-n. Aluminophosphate ($AlPO_4$) molecular sieves'framework is electrically neutral without ion exchange capability. Introduction of silicon atoms into their structure causes a negative imbalance in the framework's charge. Hydroxyl groups as Bronsted acidic sites are formed by neutralization of the negatively charged centers with the proton left after decomposition of organic template in the calcination process [1-4].

Silicoaluminophosphate molecular sieves have considerable potential as acidic catalysts [5] which can play different key roles such as membrane or adsorbent in sorption reactions and catalyst in petrochemical reactions especially methanol-to-olefin (MTO) process that has been considered a promising technology to produce lower olefins from natural gas [6]. SAPO-34 catalyst shows an exceptional selectivity for lower olefins and the complete conversion of methanol in the MTO reaction, although it is rapidly deactivated by coke, which completely blocks the internal channels of the SAPO-34 crystals. Using SAPO-34 catalyst with small crystallite size enhances the accessibility of methanol into its cages, resulting in better catalytic performance [7-9]. Since the diffusion of methanol in the SAPO-34 catalyst is limited by its small cages, only some

Corresponding author: Rouein Halladj, e-mail: halladj@aut.ac.ir

cages near the external surface are active in the MTO reaction [10], therefore the effectiveness of the SAPO-34 catalyst is improved by reducing its crystallite size [9].

The importance of nanoparticles, especially nanocatalysis and their uses in different industries has attracted many researches. The materials in nano-scale show different characteristics in comparison with their bulk state [11,12]. Huge amount of investigations about the effect of crystal size show that the best performance for SAPO-34 catalysts of sizes less than 500 nm [13-15]. Below this diameter no diffusion limitations observed during the catalytic reaction. Hirota *et al.* [15] accomplished to synthesize nanocrystals of SAPO-34 by a dry gel conversion using tetraethylammonium hydroxide (TEAOH) as a structure-directing agent (SDA). The final product was pure SAPO-34 with average small crystal size (75 nm) which is significantly reduced in comparison with samples which previously prepared by this team by hydrothermal method using the same SDA (800 nm). Chen *et al.* [14] examined the effects of the crystal size of SAPO-34 on its selectivity and deactivation in the MTO reaction. SAPO-34 fractions with a crystal size of less than 500 nm showed an excellent lifetime in the MTO reaction. The van Heyden group [16] reported synthesis of SAPO-34 nanocrystals with diameter less than 400 nm by the use of colloidal precursor solutions in the presence of tetraethylammonium hydroxide as a template at different hydrothermal conditions carried out in conventional ovens. Also, by means of microwave hydrothermal treatment the diameter was further reduced to 100 nm, and the resultant material was fully crystalline with a well-defined cube-like morphology.

The crystallization of molecular sieves is a very complicated process. Template and silicon sources, crystallization condition and material composition in initial gel show important influences on SAPO synthesis. Organic compound, *i.e.*, template, plays the most important role on structure, crystal size and morphology [17]. The action for an organic compound in AlPO or SAPO synthesis is well known for the role of structure directing agent (SDA), space filling and charge compensating [18].SAPO molecular sieves can be prepared by various templates, however, different physicochemical properties might be observed according to the type of template and its concentration during the preparation. SAPO-34 can be synthesized with many templates such as tetraethyl ammoniumhydroxide (TEAOH), dipropylamine (DPA), diethylamine (DEA), morpholine and triethylamine (TEA), in which TEAOH is the most commonly used. Furthermore, the morphology and size of the SAPO-34 crystals are strongly influenced by silica sources due to the different solubility of silica sources in alkaline medium [19,20]. Colloidal silica, fumed silica and TEOS (tetraethylorthosilicate), as an organic source of silica, are mostly used to synthesis of SAPO-34 crystals.

In this work several samples were synthesized under hydrothermal conditions by using TEAOH, DEA, TEA, and morpholine as structure-directing agents and TEOS and fumed silica as silicon sources. The influence of template, silicon sources and crystallization condition on structure, morphology and crystal size were studied. The SAPO crystals were characterized by X-ray diffraction (XRD), scanning electron microscopy (SEM), energy dispersive X-ray analysis (EDAX), thermogravimetric analysis (TGA) and nitrogen adsorption technique (BET).

2. EXPERIMENTAL

2.1. Sample preparation

The silicoaluminophosphate (SAPO) molecular sieves were synthesized by hydrothermal method using precursor gel with different molar ratios that are shown in Table 1. The sources for Al and P were Aluminum isopropoxide [98% Al $(OPr^i)_3$, Merck] and H_3PO_4 [85 wt.% aqueous solution, Merck] respectively. Tetraethylammonium hydroxide [TEAOH, 20 wt.%, Aldrich], morpholine [99 wt.%, Merck], diethylamine [DEA, 99 wt.%, Merck] and triethylamine [TEA, 99 wt.%, Merck] were used as SDAs. Fumed silica and tetraethyl orthosilicate (TEOS) were chosen as silica sources for preparing primary gels.

Aluminum isopropoxide was firstly mixed with template (TEAOH, DEA, TEA or morpholine) and deionized water and stirred for an hour. Silica source (TEOS or fumed silica) was then added. Finally, with continuous stirring, phosphoric acid (85 wt.% in water) was added dropwise to the above solution. The initial gel was further stirred and then placed in a 30 ml Teflon-lined stainless steel autoclave. The crystallization was conducted in an oven at a specified temperature and time. The synthesis conditions of different samples are given in Table 2.

The solid product was recovered and washed three times by centrifuging with distilled water, and then dried at 110 °C. The as-synthesized crystals were calcined at 560 °C in air for 5 h to remove the organic template molecules.

Table 1. Molar composition in synthesis gel of different samples.

Sample No.	Template	Al_2O_3	P_2O_5	SiO_2	H_2O
S1-S5	2	0.5	1	0.3	70
S6-S7	2	1	1	0.6	70
S8-S10	4	1	1	0.6	70
S11-S13	2	1	1	0.6	70
S14	4	1	1	0.6	70

2.2. Characterization

Powder X-ray diffraction (XRD) patterns were recorded in step scanning on a Philips PW3050 X-ray diffractometer by using CuKα radiation (λ = 1.54 Å) operating at 40 kV and 40 mA. The crystal morphology and crystal size were analyzed by scanning electron microscopy (SEM, Philips XL30 30 kV). The chemical composition of calcined samples was determined by energy dispersive X-ray analyzer (EDX, Philips XL30 30 kV). Thermo-gravimetric analysis (TGA) was performed to detect the thermal decomposition of amine templates of as-synthesized catalysts using TA instrument (TGA-50, Shimadzu) under an air flow (100 mL/min) at a heating rate of 20 °C/min from room temperature up to 900 °C. The BET surface areas of calcined samples were determined from isotherm data of nitrogen adsorption data in the relative pressure (*P*/*P*0) range of 0.05–0.30 obtained at 77.35K using Autosorb-1Quantachrome analyzer.

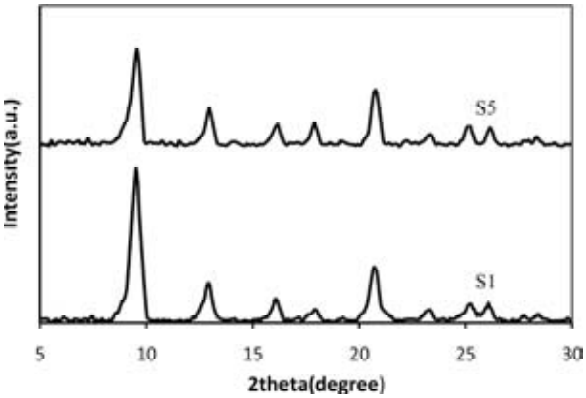

Fig. 1. XRD patterns of the samples synthesized using TEAOH as template with different silicon sources. S1: TEOS, S5: Fumed silica.

3. RESULTS AND DISCUSSION

3.1. Effect of the template source

Crystallization process in the synthesis of SAPO crystals depends significantly on the type of SDA, because both the nucleation and crystal growth rates related to the alkalinity of the solution and the interaction between the SDA and the inorganic species. In our study, TEAOH, DEA, TEA, and morpholine were used as templates for preparation of samples. TEOS and fumed silica were chosen as silica sources as well.

The XRD patterns of the samples prepared by different templates are shown in Figs. 1-4. The XRD patterns of all the synthesized samples match well

Table 2. Synthesis conditions of different samples.

Sample No.	SDA	Silica source	Temperature (°C)	Time (hr)	Phase
S1	TEAOH	TEOS	200	24	SAPO-34
S2	TEAOH	TEOS	200	14	SAPO-34
S3	TEAOH	TEOS	200	6	SAPO-34
S4	TEAOH	TEOS	200	3	Amorphous
S5	TEAOH	Fumed silica	200	24	SAPO-34
S6	Morpholine	TEOS	200	24	SAPO-5+SAPO-34
S7	Morpholine	fumed silica	200	24	SAPO-5+SAPO-34
S8	Morpholine	TEOS	200	24	SAPO-34
S9	DEA	TEOS	200	24	SAPO-34
S10	DEA	fumed silica	200	24	SAPO-34
S11	DEA	TEOS	200	24	SAPO-34+ Cristobalite+ Augelite
S12	TEA	TEOS	200	24	SAPO-5+SAPO-34
S13	TEA	fumed silica	200	24	SAPO-5+SAPO-34
S14	TEA	TEOS	200	24	SAPO-5+SAPO-34

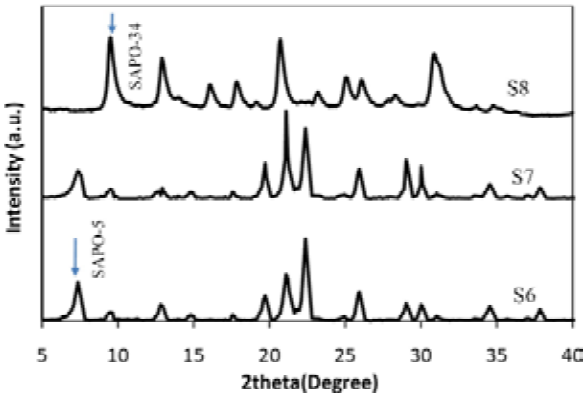

Fig. 2. XRD patterns of the samples synthesized using morpholine as template with different silicon sources.S6: TEOS, S7: Fumed silica, S8: TEOS (doubled concentration of morpholine).

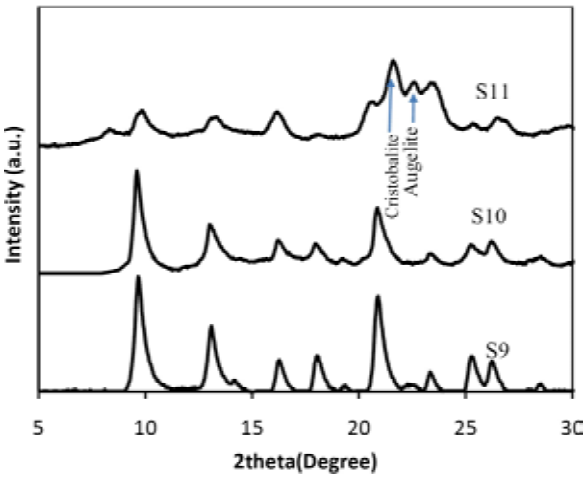

Fig. 3. XRD patterns of the samples synthesized using DEA as template with different silicon sources. S9: TEOS (doubled concentration of DEA), S10: Fumed silica (doubled concentration of DEA), S11: TEOS.

with those of SAPO-5 and SAPO-34 structures reported in the literature [21]. As seen in Table 2, crystallization time and temperature for these samples are 24 h and 200 °C, respectively. The intensity and position of each peak differs according to the type

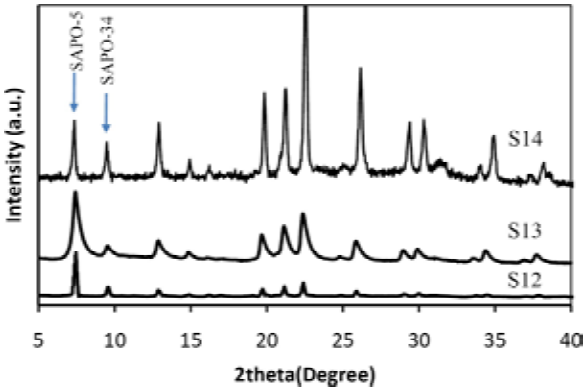

Fig. 4. XRD patterns of the samples synthesized using TEA as template with different silicon sources .S12: TEOS, S13: Fumed silica, S14: TEOS (doubled concentration of TEA).

and amount of template. It reveals that samples with the same crystallization condition but using different templates possess different crystal phase and purity, even though different silicon sources have no effect on the crystal phase and structure.

Fig. 1 shows XRD patterns of the samples synthesized using TEAOH as template agent. Typical powder diffraction patterns corresponding to the CHA structure of SAPO-34 could be observed for both samples prepared by TEOS and fumed silica. The crystallinity of the product S1, however, seems to be higher than sample S5 that it can be also confirmed by SEM image (Fig. 5). Yun-Jo Lee *et al.* [17] claimed that by using TEAOH as SDA, the major product was SAPO-5, though according to our experiments and other literatures [15,16], TEAOH leads mainly to SAPO-34. Van Heyden team in 2008 [16] reported synthesis of SAPO-34 nanoparticles with diameters less than 400 nm by taking advantage of colloidal precursor solutions in the presence of tetraethylammonium hydroxide as the template. In addition, Hirota *et al.* [15] accomplished to synthesize nanocrystals of SAPO-34 by

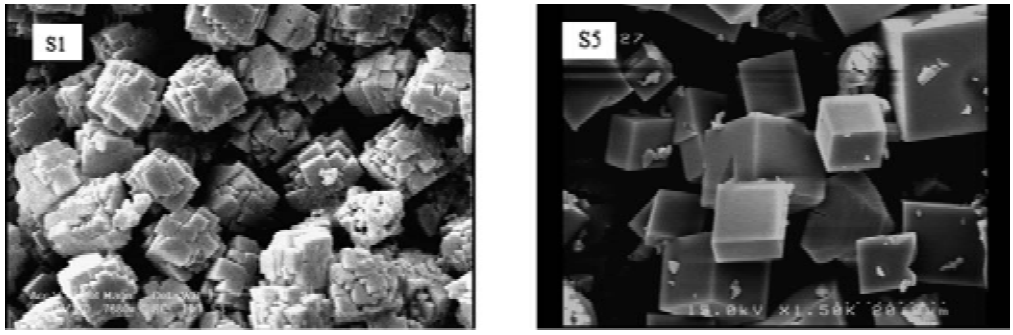

Fig. 5. SEM images of the samples synthesized using TEAOH as template with different silicon sources.S1: TEOS, S5: Fumed silica.

Table 3. Elemental compositions of calcined samples obtained by EDX analysis.

Sample No.[a]	Compositions (mol. %)				
	Si	Al	P	Si/Al in product	Si/Al in gel
S1	17.85	22.03	60.12	0.81	0.3
S2	18.98	27.96	53.06	0.68	0.3
S3	18.08	28.37	53.56	0.64	0.3
S5	4.14	19.62	76.25	0.21	0.3
S6	21.00	40.29	38.70	0.52	0.3
S7	19.70	40.04	40.26	0.49	0.3
S8	20.18	36.42	43.40	0.55	0.3
S9	19.47	37.67	42.86	0.52	0.3
S10	18.81	37.49	43.70	0.50	0.3
S11	18.19	35.45	46.36	0.51	0.3
S12	19.08	38.77	42.15	0.49	0.3
S13	20.57	42.46	36.97	0.48	0.3
S14	20.73	37.58	41.69	0.55	0.3

a: according to Table 2.

a dry gel conversion using tetraethylammonium hydroxide (TEAOH) as a structure-directing agent (SDA).

When morpholine is used as SDA, the crystalline phase of as-synthesized samples with the gel molar composition of $1.0Al_2O_3$: $1.0P_2O_5$: $0.6SiO_2$: 2.0 Morpholine: $70H_2O$ (Samples S6 and S7) is found to be significantly different as seen in Fig. 2. Major product is SAPO-5 with presence of minor one, i.e. SAPO-34. This result is contrast with that of obtained by Yun-Jo Lee *et al.* [17], where using morpholine as a template agent with the same concentration, *i.e.* 2.0 Morpholine, led to pure SAPO-34. The concentration of morpholine in initial gel seems to be very effective, because when the concentration of morpholine is doubled (Sample S8), phase transformation from SAPO-5 (AFI) to SAPO-34 (CHA) is observed. Therefore, the concentration of template agent has significant effect on phase determination [22]. Qian Wang *et al.* [23] investigated the effects of template concentration and crystallization time on the physicochemical properties of SAPO-34. The crystallinity and morphology of SAPO-34 were influenced by the concentration of the template. At low-TEA concentration, the product was cocrystallized with $AlPO_4$ and SAPO-5, and the morphology of the crystal was irregular. Pure SAPO-34 was obtained at the TEA/Al_2O_3 molar ratio of more than 2.0. The relative crystallinity, crystal size and surface area were greatly enhanced with TEA concentration.

A similar result is obtained by using DEA as SDA, in which different concentration of SDA used in initial gels leads to phase transformation (Fig. 3). XRD patterns of sample S9 and S10 show pure SAPO-34 crystals, using TEOS and fumed silica respectively, with gel molar composition of $1.0Al_2O_3$: $1.0P_2O_5$: $0.6SiO_2$: 4.0 DEA: $70H_2O$. In contrast, by reducing the template concentration (sample S11) the crystalline phase is found to be quite different from others, in which there are multiple components. A significant part of SAPO-34 is transformed to two other dense phases of $AlPO_4$ structure called Cristobalite and Augelite with strong reflections at 2θ = 21.7and 2θ = 22.2, respectively. This phase transformation reduces the intensity of the characteristic peak of SAPO-34 at 2θ = 9.6. The observed phase transformation indicates that SAPO-34 framework with low template content is unstable, because pure SAPO-34 samples (S9, S10) are obtained at the same crystallization conditions.

SAPO-5 crystals are obtained when TEA is used as a template with using both TEOS (Sample S12) and fumed silica (Sample S13) as silica sources (Fig. 4). SAPO-34 as minor phase can be seen from XRD patterns. When the concentration of SDA increases (Sample S14) no distinguishable phase transformation is observed. However sharper peaks suggest that the crystallinity increases by increasing SDA concentration. Moreover by increasing the concentration, the SAPO-34 peaks seem to be stronger. Triethylamine is basically used as a template for SAPO-5 synthesis [24,25] as seen in our existing work, whereas, it have been successfully applied instead of TEAOH as a cheap template in the synthesis of SAPO-34 [17,26], owing that

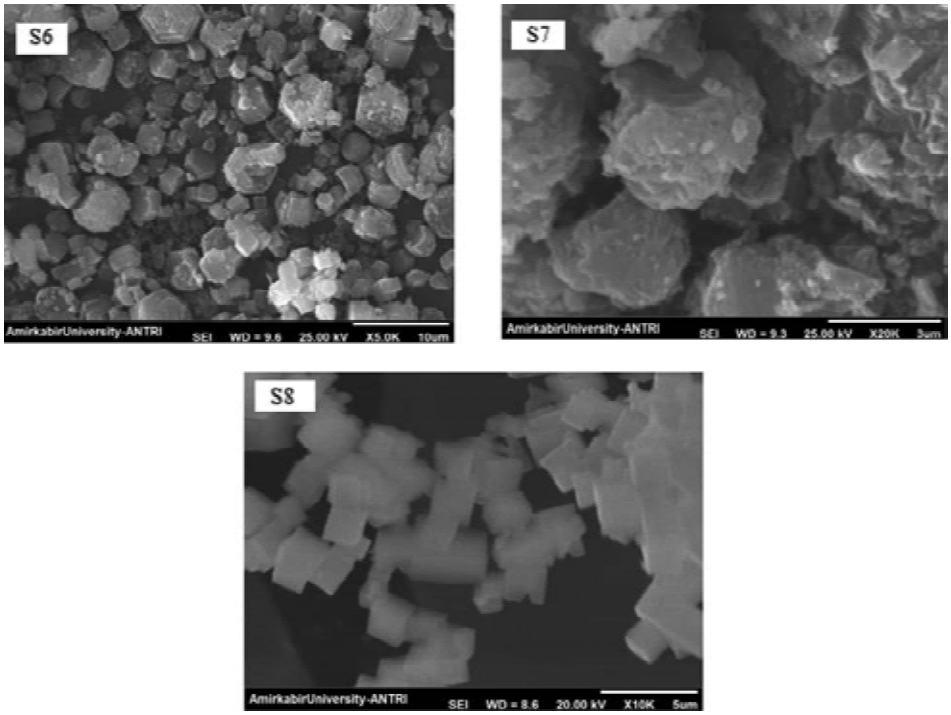

Fig. 6. SEM images of the samples synthesized using morpholine as template with different silicon sources.S6: TEOS, S7: Fumed silica, S8: TEOS (doubled concentration of morpholine).

TEAOH is an expensive reagent, and using this will result in an increase in the cost for the production of the catalysts.

By all given above, it can be concluded that forming the CHA (SAPO-34) or AFI (SAPO-5) structures depend extremely on the template source. Also CHA and AFI structures compete and the content of CHA increases with an increase in concentration of template. Based on this reason, with increasing the concentration of morpholine, phase transformation from AFI to CHA is occurred. The same results were obtained in literatures [27–29]. Also it is shown that with using different templates, different amount of Si is incorporated into the framework of SAPO molecular sieves and same crystal morphology and physicochemical properties are affected by the kinds of templates. Moreover, the CHA content increases with increasing the PH and the concentration of heteroatoms incorporated in the molecular sieves (such as Mg, Co, Si *etc.*) [30,31].

To determine the substitution degree of Si atom in the frameworks, the elemental compositions of the samples with different template and silica source, *i.e.* S1-S14, obtained by EDX technique are given in Table 3. It is found that the silicon distribution is dependent on the choice of template used during the synthesis. As shown, silicon to aluminum ratio of all samples is higher than that of the gel mixture which means more amounts of Si and/or remained as amorphous silica phase on extra-framework. While this ratio for samples S1, S2, S3 that were synthesized with TEAOH as SDA is much higher than that of others, indicating that using TEAOH as SDA leads to higher incorporation of Si in SAPO frameworks. Very lower amount of silicon than the target value in final product of sample (S5) however, shows that incorporation of larger amount of silicon in SAPO-34 framework faces some difficulties at least with the present recipe. Table 3 shows that the Si to Al ratio of samples prepared by TEA (S14) and morpholine (S8) increases with increasing in concentration of template. This implies that phase transformation from AFI to CHA occurred with increasing in Si amount incorporated, even though this result is not consistent with that for Mor/TEAOH synthesis of SAPO-34 by Yun-Jo Lee *et al.* [17], which was reported that the reduction of Si content during synthesis of gel to half under the same synthesis conditions led to the formation of only pure SAPO-34 phase.

Figs. 5-8 show SEM images of synthesized samples prepared by different templates. It is clear that different morphology and crystal size are obtained. Among the samples synthesized by TEOS as silicon source, sample S1, shows spherical aggregates of nano-sized (400–750 nm) cube type SAPO-34 crystals where the aggregates show average crystal size of 2 μm with homogeneous size

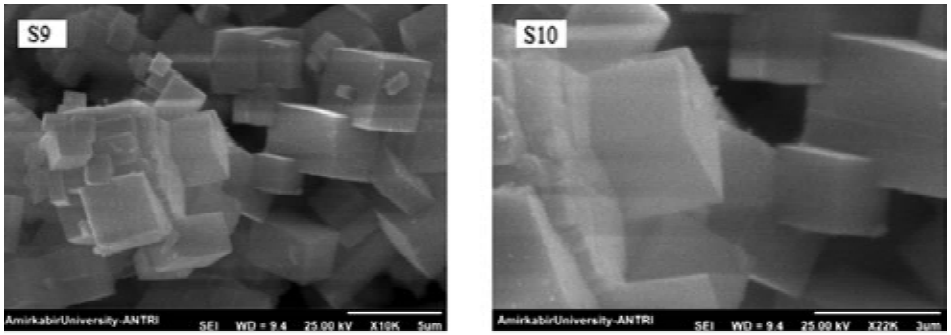

Fig. 7. SEM images of the samples synthesized using DEA as template with different silicon sources.S9: TEOS, S10: Fumed silica.

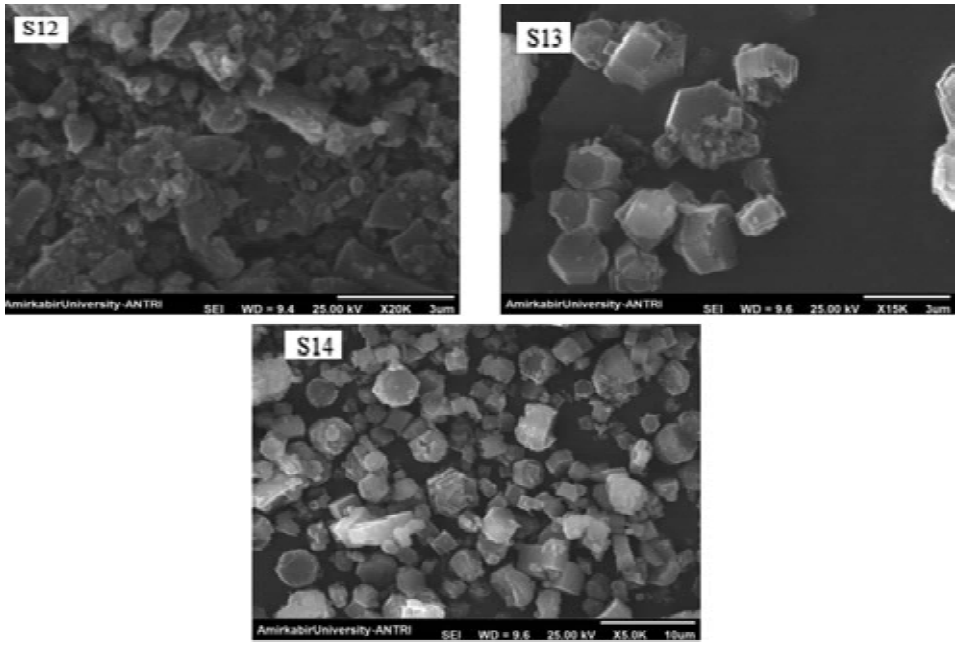

Fig. 8. SEM images of the samples synthesized using TEA as template with different silicon sources.S12: TEOS, S13: Fumed silica, S14: TEOS (doubled concentration of TEA).

distribution (Fig. 5). According to the research done by Yun-Jo Lee *et al.* [17] M15 sample (with morpholine and TEAOH amounts in gel composition; 1.5 morpholine: 0.5 TEAOH), showed spherical aggregates of nano-sized cube type SAPO-34 crystals where the aggregates showed average crystal size of 1 μm. On the contrary, bigger crystals of SAPO-34 with different size of 1-4 μm, are formed by using DEA (Sample S9) as SDA as shown in Fig. 7. In the case of SAPO-34 synthesized by Liping Ye *et al.* [32] with single TEAOH, homogeneous crystals with small particle size of 0.3–0.8 μm were obtained. By contrast, big crystals with different size, ranging broadly from 3.1 to 9.1 μm, were formed in the case of SAPO-34 synthesized with DEA only. This result means that the rate of crystal growth varied closely with the type of SDAs in the initial gel. Interestingly, as the molar content of DEA increased in the gel, a simultaneous increase of the crystal size was observed.

SEM results in Fig. 6 display that the sample synthesized with the morpholine (S6) is constituted of irregular crystal particles with some hexagonal crystals and rarely cubic-like morphology, which is typical for SAPO-5 and SAPO-34 crystals respectively. By increasing the template concentration, crystals of exclusively cubic shape are observed with average crystal diameters of 2 μm for the sample S8 indicating the phase transformation from AFI to CHA as confirmed by XRD patterns. With using TEA as SDA (S12) smaller irregular crystal particles (300-900 nm) are obtained comparing to that of obtained by using morpholine (S6). Although by increasing the TEA concentration (S14) more regular particles with both hexagonal and rarely cube type morphology are found (Fig. 8).

In the case of samples synthesized by using fumed silica, SEM images of samples S5 and S10 exhibit the rhombohedral shape of typical SAPO-34. Despite their similar crystalline shape, their

crystallite sizes differ and smaller cubic crystal is observed for samples S10 comparing to sample S5. This result means that the rate of crystal growth varied closely with the type of SDAs and silicon in the initial gel and the interaction between them. Consequently, the nature of template used in synthesis, not only influences the products structure and crystal phase, but also determines the morphology and crystal size of final crystals due to different rate of crystal growth.

The TGA profiles of samples S1, S8, S9, and S14 are described in Fig. 9. TG results show three weight losses (I, II, III) in the range of 50–800 °C. The first weight loss (I) in the low temperature range of 50–200 °C with an endothermic process is attributed to the water desorption from the sample. The second weight loss (II) between 200 and 550 °C with a strongly exothermic process is due to the combustion decomposition of template. The third weight loss (III) at temperature higher than 550 °C with an exothermic process is likely associated with the further removal of organic residue occluded in the channels and cages of SAPO. The TG curves of the samples S9 and S14 show similar patterns with weight losses in the temperature ranges of 50–200, 200–550, and 700-800 °C that it can be related to close structural forms of templates DEA and TEA. The TGA study indicates that complete decomposition of template occurs at temperatures greater than 500 °C. Hence the calcination was carried at the said temperature during the present investigation.

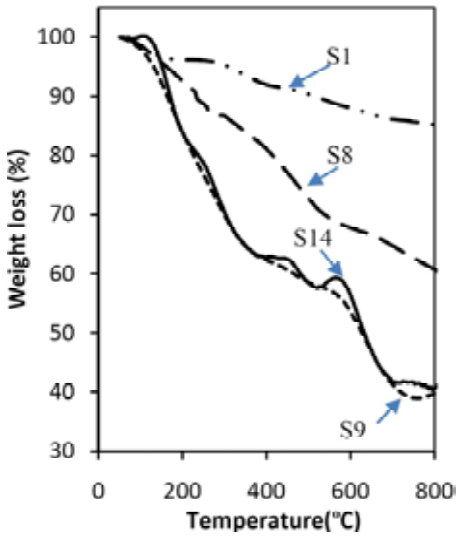

Fig. 9. TGA analysis of as-synthesized samples S1, S8, S9, and S14.

3.2. Effect of silica source

The most influential of synthesis parameters on crystal size and distribution is found to be the choice of silica source. Fumed silica and TEOS, as an organic source of silica, were used to investigate the influence of silica source material on the SAPO crystallization, size and shape of crystallites. The fumed silica is introduced to the reaction mixture in its solid form; therefore its solubility plays an important role during the synthesis whereas the organic phase can dissolve TEOS and then it can be hydrolyzed in aqueous phase.

With each template agent, SAPO crystals were synthesized with two different silica sources as shown in Table 2. When TEAOH is used as a template (samples S1, S5), SAPO-34 cubic crystals with size of 5–15 mm are formed using fumed silica as silica source, whereas smaller cube type aggregated crystals with average crystal size of 600 nm are found by using TEOS (Fig. 5), indicating that the presence of fumed silica had little effect on the morphology but did accelerate greatly the crystal growth of SAPO-34. Also, narrower size distribution obtained by using TEOS as silica source, whereas using fumed silica leads to wider particle size distribution. Lin *et al.* [33] fabricated SAPO-34 nanoparticles with controlled shape and size through choosing various source of silica, under microwave radiation. Using both of the colloidal silica and solid SiO_2 powder resulted in same product, *e.g.* SAPO-34 crystals with sheet-like morphology but a little more aggregated in the sample which was prepared using SiO_2 powder as the silica source. Also, substitution of tetraethyl orthosilicate for colloidal silica or SiO_2 powder changed the morphology of particles to a shape of irregular spheres significantly and produced uniform nanoparticles with sizes of about 100 nm.

In the case of morpholine as a template (samples S6, S7), different morphology are obtained as shown in Fig. 6. A mixture of hexagonal and cubic or rhombohedral crystals with average particles size of 2 μm and irregular shape crystals with average particles size of 3 μm are obtained by using TEOS and fumed silica respectively.XRD pattern in Fig. 2 shows that the degree of crystallinity for both samples S6 and S7 are almost the same. These results demonstrate that TEOS as the silicon source could lead to finer particles, but has more or less no effect on crystallinity of SAPO-5 molecular sieve.

Very smooth cube like SAPO-34 crystals (S9, S10) are obtained by using DEA with both TEOS and fumed silica (Fig. 7), although using TEOS gives almost smaller particles.

Table 4. BET results for samples with different crystallization time.

Sample No.[a]:	S1(24h)	S2(14h)	S3(6h)
S_{BET} (m^2gr^{-1}) :	366.5	363.5	240.02

a: according to Table 2.

With using TEA as SDA, crystals with 300-900 nm in size are formed by using TEOS as silica source (S12), while 1.5-2.5 mm particles were found by using fumed silica (S13). Similar to previous results, TEOS gives finer crystals compared with that of fumed silica (Fig. 8).

These morphology changes revealed that the effect of different silica sources plays a crucial role in the shape and size control of SAPOs crystals due to different solubility and reactivity rate of silica sources. Indeed, the same phenomenon that silica source influences the particle size of other zeolites, for example silicalite-1, has already been reported which demonstrates that crystals formed by using TEOS as silica source are much smaller than those obtained by other silica sources [34].

3.3. Effect of crystallization time

Four samples (S1-S4) with different crystallization time were synthesized to study the effect of this parameter on crystallite size, crystallinity and morphology. The powder XRD patterns of samples (the gel molar composition is $0.5Al_2O_3$: $1.0P_2O_5$: $0.3SiO_2$: 2.0TEAOH: $70H_2O$) are shown in Fig. 10. The XRD pattern of the sample are crystallized for 3 h demonstrates that the sample mainly consists of the amorphous phase. However, very weak peaks emerge at $2\theta = 9.5°$ and 20.5°, suggesting the appearance of a very small amount of SAPO-34 crystals. It can be confirmed from SEM image for sample S4, (Fig. 11) that is shown the existence of a large amount of amorphous phase of undefined morphology with thimbleful cubic-like crystals of SAPO-34.

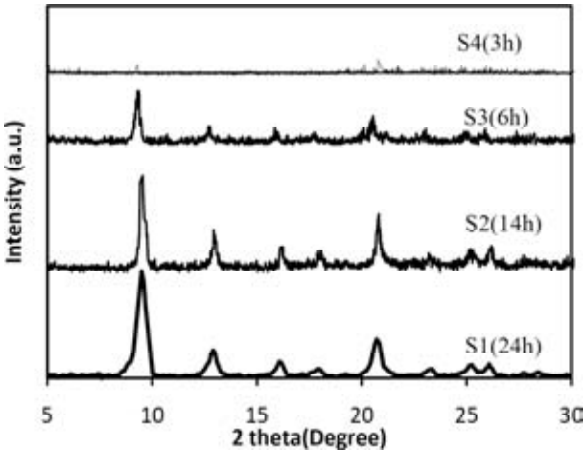

Fig. 10. XRD patterns of the samples synthesized with different crystallization time at crystallization temperature of 200 °C.

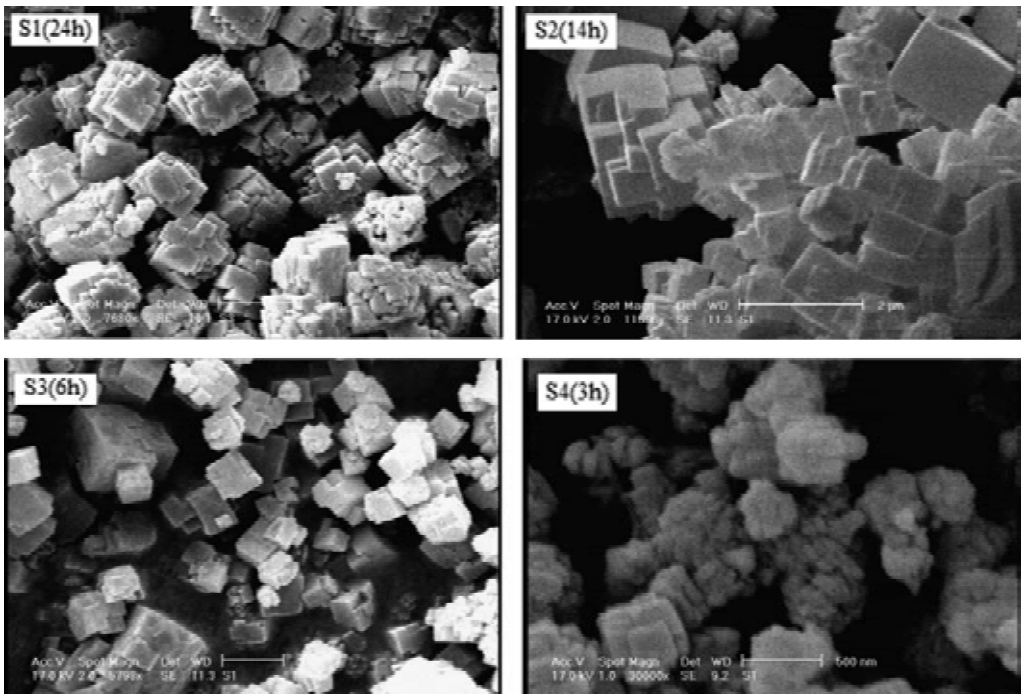

Fig. 11. SEM images of as-synthesizad samples with different crystallization time.

The diffraction peaks of SAPO-34 become evident after 6 h and the amorphous phase almost disappears when the samples are crystallized for more than 14 h. The crystallinity further increases with crystallization time and a fast transformation of the crystalline phase is observed. Also, the crystallinity reaches the highest amount at 24 h. The relative crystallinity of 100, 90, 60, and 3% are observed for samples S1, S2, S3, and S4, respectively, based on XRD peak intensity of peak appearing at 2θ = 9.5°.

Generally, SAPO-34 crystals grow larger and larger with the crystallization time. Because aggregation to form large pseudo-spherical particles happens quickly after crystal nuclei formation, controlling the suitable crystallization time is a key factor in obtaining SAPO-34 with small crystals. As seen in Fig. 11 the average crystal size of 400, 500, and 600 nm are obtained for the samples synthesized at crystallization times of 6, 14, and 24 h, respectively. However spherical aggregates of 600 nm cube type SAPO-34 crystals are formed for crystallization time of 24 h, where the aggregates showed average crystal size of 2 μm with homogeneous size distribution. The same results were obtained by Qian Wang *et al*. [23] where before 2 h crystallization time, the relative solid yield was low. A fast increase in the yield was observed with the crystallization time from 2 to 11 h. The solid yields were influenced by the counteraction parameters between the dissolution of amorphous alumina into the solution and the generation of crystals. After 11 h, the yield still increased with a much flatter slope. Nishiyama *et al.* [9] showed that the crystal size increased with increasing crystallization time. The SAPO-34 sample after 24 h was very uniform with crystals of about 800 nm in size. However, the samples in the early stages of the synthesis contained amorphous particles.

According to the results above, it can be concluded that during the synthesis process of SAPO-34 molecular sieves, after the formation of crystal nuclei, they are capable of aggregating quickly to form large pseudo-cubical particles. Thus, controlling the suitable crystallization time and careful adjustment of synthesis conditions is a way to obtain SAPO-34 crystals with small size.

EDX results of Table 3 show that with increasing the crystallization time, the silicon to aluminum molar ratio increased.

BET surface area of the samples with different crystallization time measured by nitrogen adsorption experiment is listed in Table 4. Considering samples S3 to S1 in order, we see an increase in crystallite size and crystallinty .Consequently, increasing the crystallization time of the samples leads to the rises in the surface areas from 240.02 to 366.5 m^2g^{-1}. In the case of samples S3, the surface area is significantly lower than that of S1, S2.This observation strongly suggests that with decreasing crystallization time the sample partially lost its crystallinity and it become amorphous. This result is consistent with XRD patterns discussed earlier where crystallinity is found to be increased with increasing crystallization time. This result accords well with the data obtained by Qian Wang *et al.* [23], which showed that the surface area increases gradually with increasing the template concentration, since the crystallinity of SAPO-34 enhances, and the impurity phase disappears.

4. CONCLUSIONS

Synthesis of SAPO crystals with small crystallite size, which has been considered as a challenging task to date, was successfully performed under static conditions during crystallization. The effects of template, silicon sources and crystallization time on crystal phase, morphology, crystal size and crystallinity were investigated and the results were compared with those of obtained from other investigations reported in this field. The products were characterized by XRD, SEM, EDX, BET and TGA. The XRD patterns reveal that samples with the same crystallization condition but using different templates produce different crystal phase and purity, even though different silicon sources have no effect on crystal phase and structure. Yun-Jo Lee *et al.* [17] claimed that by using TEAOH as SDA, the major product will be SAPO-5, though according to our experiments and other literatures [15,16], TEAOH leads mainly to SAPO-34. Also, the results show that TEA is an appropriate template for synthesis of SAPO-5. The concentration of SDA is a crucial factor when DEA or morpholine is used. The more the concentration of morpholine, results in phase transformation from AFI to CHA .That is comparable to that of obtained by Qian Wang *et al.* [23] where with increasing the template concentration, phase transformation occurred. Using TEOS as silica source, results in finer particles with narrower size distribution for almost all samples. In particular, nano-sized crystals obtained by using TEOS as silica source with both TEAOH and TEA as SDAs. According to our work and other researches, Crystallization time has a significant effect on crystal size and crystalliniy. Amorphous phase obtains at the early stage of crystallization time. The crystal

size increased with increasing crystallization time. Afterward, the crystallinity level off and the crystal size become larger.

REFERENCES

[1] F.J. Keil, J .Hinderer and A.R. Garayhi // *Catal Today* **50** (1999) 637.

[2] E. Furimsky, *Catalysts For Upgrading Heavy Petroleum Feeds* (Elsevier Science B.V., Amsterdam, 2007).

[3] J. A Martenes, I. Balakrishnan, P. J Grobet and P. A. Jacob, *Zeolite Chemistry And Catalysis* (Elsevier Science B.V., Amsterdam, 1991).

[4] Z. Liu and J. Liang // *Current opinion in solid state and materials science* **4** (1999) 80.

[5] S. Rajiv, D.G. Julian and C.P. Michael // *Phase Transition* **61** (1997).

[6] N. Fatourehchi, M. Sohrabi, S.J. Royaee and S.M. Mirarefin // *Chemical Engineering Research and Design* **89** (2011) 811.

[7] Y. Hirota, K. Murata, M. Miyamoto, Y. Egashira and N. Nishiyama // *Catal Lett* **140** (2010) 22.

[8] Y.H. Song, H.J. Chae, K.E. Jeong, C.U. Kim, C.H. Shin and S.Y. Jeong // *J. Korean Ind. Eng.Chem.* **19** (2008) 559.

[9] N. Nishiyama, M. Kawaguchi, Y. Hirota, D.V. Vu, Y. Egashira and K. Ueyama // *Appl.Catal. A: Gen* **362** (2009) 193.

[10] B.P.C. Hereijgers, F. Bleken, M.H. Nilsen, S. Svelle, K.-P. Lillerud, B.M. Weckhuysen and U. Olsbye // *J. Catal.* **264** (2009) 77.

[11] S. Askari, R. Halladj and B. Nasernejad // *J. Mater. Sci-Poland.* **27** (2009) 397.

[12] J. Talebi, R. Halladj and S. Askari // *J. Mater. Sci.* **45** (2010) 3318.

[13] M. Razavian, R. Halladj and S. Askari // *Rev. Adv. Mater. Sci.* **29** (2011) 83.

[14] D. Chen, K. Moljord, T. Fuglerud and A. Holmen // *Micropor. Mesopor. Mater.* **29** (1999) 191.

[15] Y. Hirota, K. Murata, S. Tanaka, N. Nishiyama, Y. Egashira and K. Ueyama // *Mater. Chem. Phys.* **123** (2010) 507.

[16] H. van Heyden, S. Mintova and T. Bein // *Chem. Mater.* **20** (2008) 2956.

[17] Y.J. Lee, S. C Baek and K.W Jun // *J. Appl. Catal. A*. **329** (2007) 130.

[18] R. Vomscheld, M. Briend, M.J. Peltre, P.P. Man and D. Barthomeuf // *J. Phy. Chem.* **98** (1994) 9614.

[19] Y.J. Wu, X.Q. Ren, Y.D. Lu and J. Wang // *Microporous Mesoporous Mater* **112** (2008) 138.

[20] M. Mertens and K.G Strohmaier, *US Patent 6696032 B2* (2004).

[21] B.M. Lok, C.A. Messina, R.L. Patton, R.T. Gajek, T.R. Cannan and E.M. Flanigen, *US Pat. 4440871*, (1984).

[22] G. Liu, P. Tian, J. Li, D. Zhang, F. Zhou and Z. Liu, *Microporous Mesoporous Mater.* **111** (2008) 143.

[23] Q. Wang, L. Wang, H. Wang, Z. Li, H. Wu, G. Li,X. Zhang and S. Zhang // *Asia-Pac. J. Chem. Eng*. (2010)

[24] S.H. Jhung, J.-S. Chang, J.S. Hwang and S.-E. Park // *Micropor. Mesopor. Mater.* **64** (2003) 33.

[25] S.H. Jhung, J.-H. Lee, J.W. Yoon, J.-S. Hwang, S.-E. Park and J.-S. Chang // *Micropor. Mesopor. Mater.* **80** (2005) 147.

[26] Z. Liu, C. Sun, G. Wang, Q. Wang and G. Cai // *Fuel Process. Technol.* **62** (2000) 161.

[27] P. Concepcion, J.M.L. Nieto, A. Mifsud and J. Perez-Pariente // *Zeolites* **16** (1996) 54.

[28] C. He, Z. Liu, L. Yang and G. Cai // *Tianranqi Huagong* **18** (1993) 14.

[29] Y. Xu, J. Maddox and J.W. Couves // *J. Chem. Soc. Faraday Trans.* **86** (1990) 425.

[30] U. Lohse, R. Bertram, K. Jancke, I. Kurzawaski, B.Parlitz, E. Löffler and E. Schreier // *J. Chem. Soc. Faraday Trans.* **91** (1995) 1163.

[31] M.G. Uytterhoeven and R.A. Schoonheydt // *Micropor. Mater.* **3** (1994) 265.

[32] Liping Ye, Fahai Cao, Weiyong Ying, Dingye Fang and Qiwen Sun // *Journal of Porous Materials* **18** (2011) 225.

[33] S. Lin, J. Li, R.P. Sharma, J. Yu and R. Xu // *Top Catal* **19** (2010) 1304.

[34] S. Mintova and V. Valtchev // *Microporous Mesoporous Mater* **55** (2002) 171.